THE DYNAMICS OF THE SPONTANEOUS ENHANCED CONFINEMENT REGIME IN THE REVERSED-FIELD PINCH

R. GATTO, P. W. TERRY, C. C. HEGNA

DEPARTMENT OF PHYSICS
UNIVERSITY OF WISCONSIN-MADISON
MADISON, WI 53706 USA

Poster DP1-0.92 of the American Physical Society - Division of Plasma Physics Meeting,
October 23-27 2000, Québec City, Canada

OBJECTIVE

STUDY OF THE TRANSITION TO THE SPONTANEOUS ENHANCED CONFINEMENT REGIME IN THE RFP

OUTLINE

- Spontaneous Enhanced Confinement Regime in RFP
- Tearing Mode Stability with Shear Flow
- Reynolds Stress and Shear Flow Generation due to Tearing Modes
- Transition Modeling

Spontaneous Enhanced Confinement Regimes in RFP

Regimes of enhanced confinement in the Madison Symmetric Torus RFP can occur spontaneously, following sawtooth crashes.

These discharges are characterized by:

- reduced electrostatic and global magnetic fluctuations, leading to improved τ_n and τ_E;
- a strong flow shear just outside the reversal radius.

- Additional experimental observations:
  - Transition occurs during sawtooth crash;
  - The generated flow is dominantly toroidal;
  - Plasma rotation slows during crash, starting first in core, then moving toward edge.
  - Increase of ∇P_e in the region of strong shear (transport barrier).

- Transition Physics:
  We postulate that:
  - The shear flow is generated by magnetic Reynolds stress during the excitement of global ($m = 1$, low n) and local ($m = 1$, high n and $m = 0$) ω_*-tearing modes in a sawtooth crash
  - After the crash, as the Reynolds stress decays, the edge flow is maintained by the steepened pressure gradient created by the suppression of turbulence

A more detailed dynamics ...

Pre-crash Phase

- $m = 1$, $n = 6 - 8$ core tearing modes (with $\omega_* \simeq 0$ since $\nabla P \simeq 0$); $\mathrm{Re}\langle \tilde{B}_{r,\mathbf{k}}\ \tilde{B}_{\phi,-\mathbf{k}} \rangle = 0$ (fluctuations out of phase).
- Small amplitude $m = 1$, high-n propagating ω_*-tearing modes closer to the reversal layer; $\mathrm{Re}\langle \tilde{B}_{r,\mathbf{k}}\ \tilde{B}_{\phi,-\mathbf{k}} \rangle \simeq 0$ (small fluctuation amplitudes).
- Plasma tends to rotate toroidally almost rigidly (the torque due to the coupling between core and edge modes slows down core modes).
- No edge rotation induced by Reynolds stress.

Crash Phase

- Sawtooth crash induced $m = 1$, low-n core tearing mode nonlinearly excite $m = 1$, high-n and $m = 0$ ω_*-tearing modes near the reversal radius; large $\mathrm{Re}\langle \tilde{B}_r\ \tilde{B}_\phi \rangle \rightarrow \langle V_{\phi,i} \rangle$ (via ion momentum balance).
- $\langle V_{\phi,i} \rangle \rightarrow \langle E_r \rangle$ (via Ohm's law).
- $\langle E_r \rangle \rightarrow \langle V_{\phi,i} \rangle$ (via $E \times B$).

Post-crash Phase

- The high-n, ω_*-tearing modes near the reversal radius lose energy, and $\mathrm{Re}\langle \tilde{B}_r\ \tilde{B}_\phi \rangle \rightarrow \simeq 0$;
- Crash-generated $\langle V_{E\times B} \rangle$ suppresses edge turbulence and steepens ∇P, which now maintains the toroidal flow (via momentum balance and Ohm's law).
- Δ' is reduced by both crash-generated $\langle V_{E\times B} \rangle$ and lower resistivity.
- Toroidal ion flow is slowly restored to pre-crash state by nonlinear torques.

Tearing Mode Stability with Shear Flow

- Ideal MHD System

$$\boldsymbol{\nabla}\cdot\mathbf{B}=0\ , \qquad \boldsymbol{\nabla}\cdot\mathbf{V}=0$$

$$\rho\left[\frac{\partial\mathbf{V}}{\partial t}+(\mathbf{V}\cdot\boldsymbol{\nabla})\,\mathbf{V}\right]+\boldsymbol{\nabla}p-\mathbf{J}\times\mathbf{B}=0\ , \qquad \mathbf{E}=-\mathbf{V}\times\mathbf{B}\ ,$$

$$\mu_0\mathbf{J}=\boldsymbol{\nabla}\times\mathbf{B}\ , \qquad \frac{\partial\mathbf{B}}{\partial t}=-\boldsymbol{\nabla}\times\mathbf{E}\ .$$

- In cylindrical geometry and assuming the following fields

$$\mathbf{B}(r,\theta,t)=\left[B_\theta(r)\hat{\boldsymbol{\theta}}+B_z(r)\hat{\mathbf{z}}\right]+\tilde{\mathbf{B}}(r)e^{i(m\theta+kz+\omega t)}$$

$$\mathbf{V}(r,\theta,t)=\left[V_\theta(r)\hat{\boldsymbol{\theta}}+V_z(r)\hat{\mathbf{z}}\right]+\tilde{\mathbf{V}}(r)e^{i(m\theta+kz+\omega t)}$$

a second order o.d.e. for $\tilde{B}_r(r)$ is obtained:

$$\frac{d^2\tilde{B}_r(r)}{dr^2}+C(r)\,\frac{d\tilde{B}_r(r)}{dr}+D(r)\,\tilde{B}_r(r)=0\ .$$

This equation governs ideal kink modes in the presence of an equilibrium flow.

• The coefficients $C,\ D$ depend on the following quantities:

$$C(r)\ , D(r) \propto \omega;\ k,\ m;\ F,\ G,\ \Omega,\ \Sigma^2$$

where

$$G(r) = \mathbf{k}\cdot\mathbf{V}_0 \qquad F(r) = \mathbf{k}\cdot\mathbf{B}_0$$
$$\Omega(r) = \omega + G(r) \qquad \Sigma(r)^2 = \rho\mu_0 G(r)^2 - F(r)^2$$

• Field and velocity equilibrium profiles for the RFP [polynomial function model *J. C. Sprott, Phys. Fluids 31 (8), p.2266, (1988)*]

• The outer region equation is solved numerically with $\omega = -G(r_{sing})$ to evaluate Δ':

$$\Delta' \equiv \left[\frac{1}{\tilde{B}_r^{\text{out}}}\frac{d\tilde{B}_r^{\text{out}}}{dr}\bigg|_{r\to 0+} - \frac{1}{\tilde{B}_r^{\text{out}}}\frac{d\tilde{B}_r^{\text{out}}}{dr}\bigg|_{r\to 0-}\right]$$

Field and Velocity Equilibrium Profiles

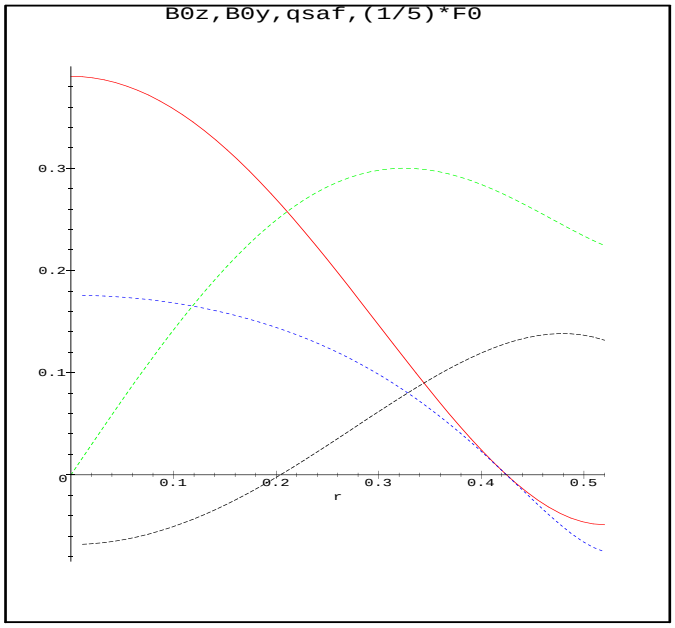

$B_t(r)$, $B_p(r)$, q(r) and $F(r)$ equilibrium profiles (PFM). Mode rational surface for the $m = 1,\ n = -7$ mode is at $r_s = 0.204$ m, while the reversal radius is at $\bar{r}_s = 0.424$ m. Units are MKSA. [F has been divided by 5 to fit the figure.]

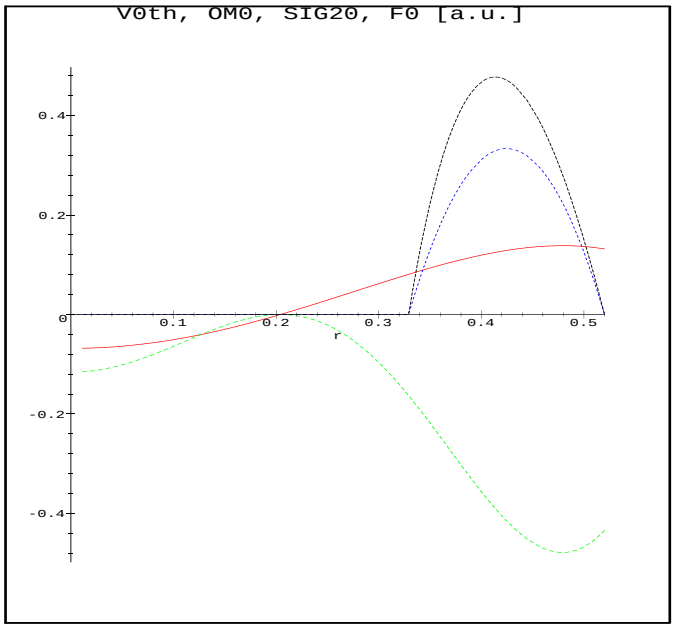

$V(r)$ (parabolic), $\Omega(r)$, $F(r)$ and $\Sigma(r)^2$ profiles.

Shear Flow is Stabilizing

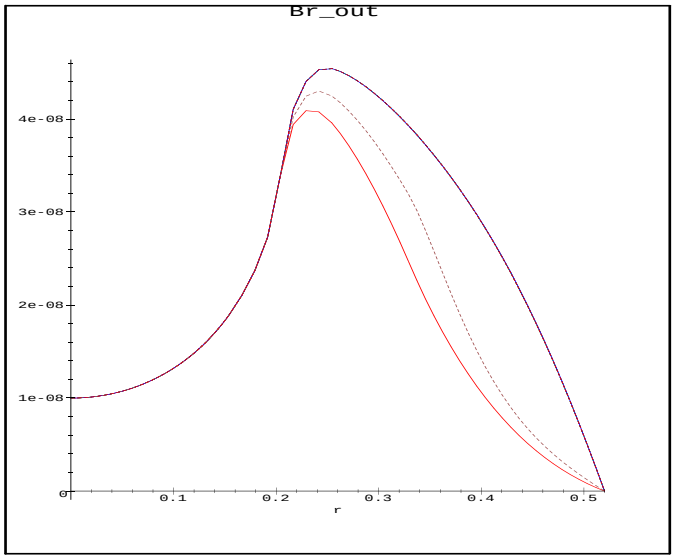

Perturbed $B_r(r)$ eigenfunctions for increasing V_0, the maximum of the parabolic velocity profile centered at the reversal radius, $\bar{r}_s = 0.42$ m.

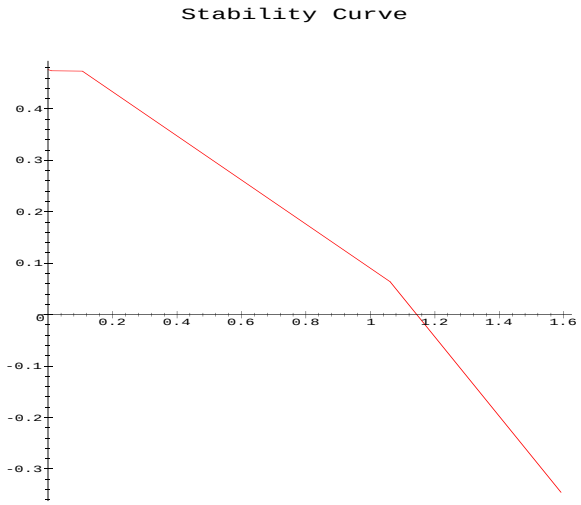

Stability parameter Δ' as a function of $(V_0/\Delta V_0)/[V_A(\bar{r}_s)/a(1 - r_s/\bar{r}_s)]$ for the parabolic $V_0 = (V_\theta^2 + V_z^2)^{1/2}$ profile study. The flow is centered at $r = \bar{r}_s$. [Here, r_s and $\bar{r}_s$ are such that $F(r_s) = 0$ and $q(\bar{r}_s) = 0$, ΔV_0 is the width of the velocity profile, a is the minor radius and V_A is the Alfvén velocity].

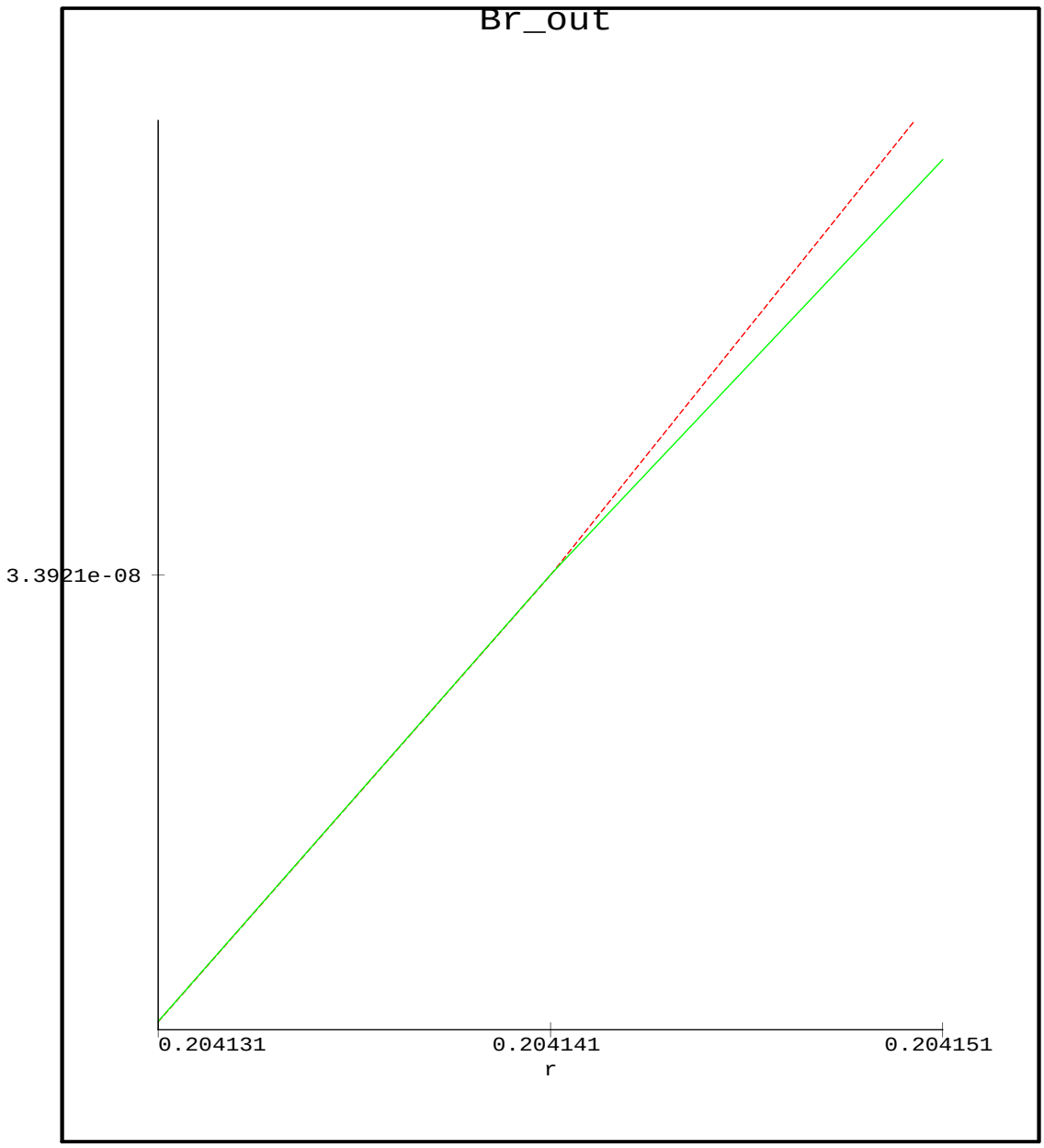

Perturbed $B_r(r)$ eigenfunctions for no shear flow (- - -) and maximum shear flow (——) around the singular surface at $r_s = 0.204$ m. The stabilizing change in slope is apparent.

Reynolds Stress and Shear Flow Generation due to Tearing Modes

- Velocity and Magnetic Reynolds Stress (quasi-linear)

$$\Re\left(\tilde{V}_x\tilde{V}_z\right) = \Re\left[i\frac{\gamma^2}{k}\tilde{\xi}\,\frac{d\tilde{\xi}}{dx}\right] \;, \qquad \Re\left(\tilde{B}_x\tilde{B}_z\right) = \Re\left[\frac{i}{k}\tilde{B}_x\frac{d\tilde{B}_x}{dx}\right]$$

- Flux surface averaged ion momentum balance

$$\frac{\partial}{\partial t}\langle V_{\phi,i}\rangle = \overbrace{-\,\mu\langle V_{\phi,i}\rangle}^{\text{viscous damping}} \overbrace{-\frac{1}{MR}(\Gamma_{in}+\Gamma_{ex})}^{\text{torques}} \overbrace{-\frac{\partial}{\partial r}\left[\langle\tilde{V}_{r,i}\;\tilde{V}_{\phi,i}\rangle - \langle\frac{\tilde{B}_r\;\tilde{B}_\phi}{4\pi\rho_m}\rangle\right]}^{\text{Reynolds stress drive}}$$

- Flux surface averaged equation for shear flow ($V'_{\phi,i} \equiv dV_{\phi,i}/dx$)

$$\frac{1}{2}\frac{\partial}{\partial t}\langle V'_{\phi,i}\rangle^2 = \overbrace{\alpha\; V'_{\phi,i}\frac{\partial^2}{\partial x^2}\left\langle\frac{\tilde{B}_x\tilde{B}_z}{4\pi\rho}\right\rangle}^{\text{Magnetic Reynolds stress drive}} + \cdots$$

• Coupled equations for the radial displacement $\tilde{\xi}_x$ and perturbed magnetic field $\tilde{B}_x$ (slab geometry)

$$\frac{d^2\tilde{\xi}_x(x)}{dx^2} = \frac{k\ B_0}{c_l^2 L_s \rho\gamma} x\ \sigma(x) \left[\frac{k\ B_0}{L_s} x\ \tilde{\xi}_x(x) + i\tilde{B}_x(x)\right]$$

$$\frac{d^2\tilde{B}_x(x)}{dx^2} = -4\pi i \frac{\gamma}{c_l^2}\ \sigma(x) \left[\frac{k\ B_0}{L_s} x\ \tilde{\xi}_x(x) + i\tilde{B}_x(x)\right]$$

• The adopted conductivity model describes the electron response to diamagnetic and shear flow effects:

$$\sigma(x) = \sigma_{\text{Spitzer}}\sigma_0(\omega)[1 - \delta(\omega)x]$$

where $\sigma_0(\omega) = (\omega - \Omega_e^*)/\omega$, $\Omega_e^* \equiv \omega_n^* + 1.71\omega_T^*$, and

$$\delta(\omega) = \frac{1.71\omega_T^* k V'}{\omega\,(\omega - \Omega_e^*)} \ll 1$$

• Perturbation expansions in $\delta_0 \simeq \epsilon \ll 1$:

$$\tilde{\xi}_x = \tilde{\xi}_0 + \delta_0\tilde{\xi}_1 + {\delta_0}^2\tilde{\xi}_2 \cdots$$

$$\omega = \omega_0 + \epsilon^2\omega_2$$

- We obtain ($\tilde{\psi} \propto \tilde{B}_x$)

$$O[(\hat{\delta}_0, \hat{\epsilon})^0] : \frac{d^2\tilde{\xi}_0(\hat{x})}{d\hat{x}^2} - \frac{\hat{x}^2}{\hat{\gamma}_0}\tilde{\xi}_0(\hat{x}) = \frac{\hat{x}}{\hat{\gamma}_0}\,\tilde{\psi}_0(x)$$

$$\frac{d^2\tilde{\psi}_0(\hat{x})}{d\hat{x}^2} - 4\pi\hat{\gamma}_0\tilde{\psi}_0(\hat{x}) = 4\pi\hat{\gamma}_0\hat{x}\;\tilde{\xi}_0(x)$$

$$O[(\hat{\delta}_0, \hat{\epsilon})^1] : \frac{d^2\tilde{\xi}_1(\hat{x})}{d\hat{x}^2} - \frac{\hat{x}^2}{\hat{\gamma}_0}\tilde{\xi}_1(\hat{x}) = \frac{\hat{x}}{\hat{\gamma}_0}\,\tilde{\psi}_1(x) - \frac{\hat{x}^3}{\hat{\gamma}_0}\,\tilde{\xi}_0(x) - \frac{\hat{x}^2}{\hat{\gamma}_0}\,\tilde{\psi}_0(x)$$

$$\frac{d^2\tilde{\psi}_1(\hat{x})}{d\hat{x}^2} - 4\pi\hat{\gamma}_0\tilde{\psi}_1(\hat{x}) = 4\pi\hat{\gamma}_0\hat{x}\tilde{\xi}_1(x) - 4\pi\hat{\gamma}_0\hat{x}^2\tilde{\xi}_0(x) - 4\pi\hat{\gamma}_0\hat{x}\tilde{\psi}_0(x)$$

etc...

- 0^{th} order: classical ω_*-tearing mode, driven by Δ';
- 1^{st} order: localized twisting mode, driven by electron dynamics.

- To solve these equations we use a Green function approach and an iteration scheme.

Velocity and Magnetic Reynolds Stress Generation

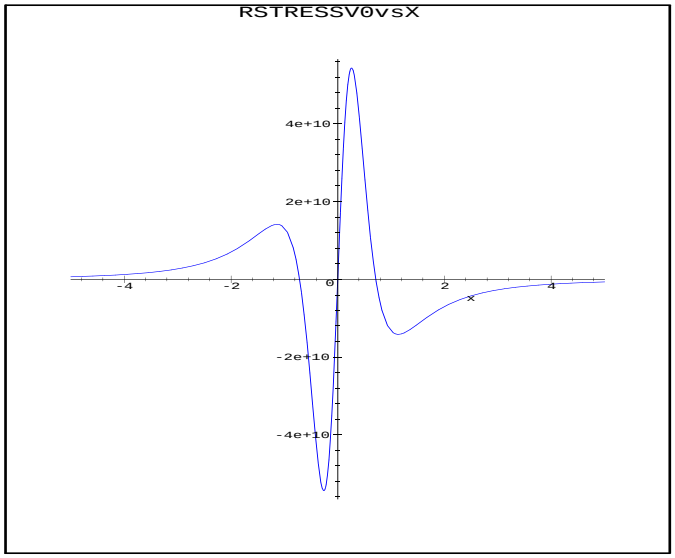

Velocity Reynolds stress (0th order).

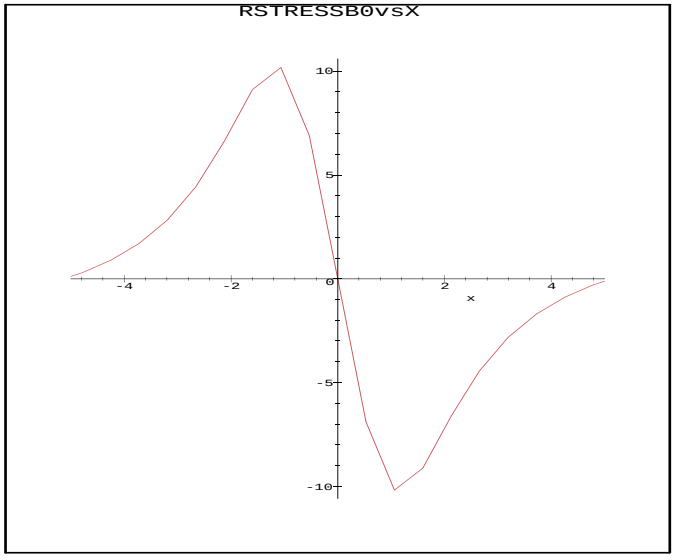

Magnetic Reynolds stress (0th order).

Flow Acceleration due to Reynolds Stress

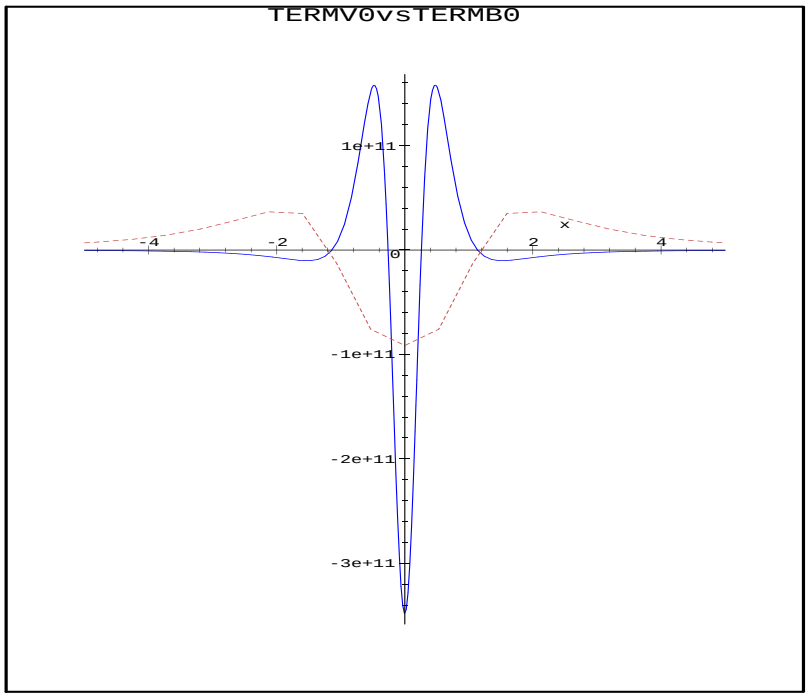

Comparison of the two driving terms associated with the 0th order Reynolds stresses [i.e., $-\partial/\partial r(\tilde{V}_{r,0}\tilde{V}_{\phi,0})$ and $+\partial/\partial r[(\tilde{B}_{r,0}\tilde{B}_{\phi,0})/(4\pi\rho_m)]$].

Transition Modeling

- Relevant equations:

  - Flux surface averaged ϕ-component of ion momentum balance

$$\frac{\partial}{\partial t}\langle V_{\phi,i}\rangle = -\mu\langle V_{\phi,i}\rangle - \frac{1}{MR}\left[\Gamma_{in}(\tilde{B}_r, V) + \Gamma_{ex}(\tilde{B}_r, V)\right] - \frac{\partial}{\partial r}\left[\langle \tilde{V}_{r,i}\ \tilde{V}_{\phi,i}\rangle - \langle \frac{\tilde{B}_r\ \tilde{B}_\phi}{4\pi\rho_m}\rangle\right]$$

  - The r-component of Ohm's law

$$\langle E_r\rangle = -\langle V_{\phi,i}\rangle\ B_{\theta,0} + \frac{m_i}{2\rho_m e}\frac{dP}{dr}$$

  - $E \times B$ toroidal drift velocity

$$\langle V_{\phi,i}\rangle = \frac{\langle E_r B_\theta\rangle}{B_0^2}$$

• Modeling system to describe the (second order) transition near the reversal radius:

$$\begin{aligned}
\frac{1}{2}\frac{\partial \mathcal{V}}{\partial t} &= -\mu_1\,\mathcal{V} + \alpha_1\,\mathcal{V}^{1/2}\,\frac{\partial^2 \mathcal{B}}{\partial r^2} \\
&\quad -\frac{\mathcal{V}^{1/2}}{MR}\frac{\partial}{\partial r}\left[\Gamma_{\rm ex}(\tilde{B}_r, \Delta V) + \Gamma_{\rm in}(\tilde{B}_r, \Delta V)\right] \\
\frac{1}{2}\frac{\partial \mathcal{B}}{\partial t} &= +\gamma_0\,\mathcal{B} - \alpha_3\,\mathcal{B}^2 - \alpha_4\,\mathcal{V}\,\mathcal{B} \\
\frac{\partial(\Delta V/R)}{\partial t} &= -\mu_2\,\frac{\Delta V}{R} + \Gamma_{\rm ex}(\tilde{B}_r, \Delta V) + \Gamma_{\rm in}(\tilde{B}_r, \Delta V)
\end{aligned}$$

where

$$\mathcal{V} = \langle V'_{\phi,i}\rangle^2$$

$$\Delta V = V_{\rm core} - V_{\rm edge}$$

$$\mathcal{B} = \langle \frac{\tilde{B}_r\ \tilde{B}_\phi}{4\pi\rho_m}\rangle$$

• The first two equations describes the evolution of shear flow and magnetic energy, while the last equation describes the evolution of the relative flow velocity of the phase-locked core tearing modes (mode deceleration occurs when the electromagnetic torques exceed the inertia and viscous forces).

Terms on the right hand sides of the equations:

- $-\mu_1\ \mathcal{V}$: frictional damping due to neoclassical and impurity effects (magnetic pumping);
- $+\alpha_1 \mathcal{V}^{1/2}\ \frac{\partial^2 \mathcal{B}}{\partial r^2}$: source due to magnetic Reynolds stress ($m = 1$, high n and $m = 0$: local modes);
- $-\frac{\mathcal{V}^{1/2}}{MR}\frac{\partial}{\partial r}\left(\Gamma_{\rm in} + \Gamma_{\rm ex}\right)$: drive terms from nonlinear internal e.m. torques and external e.m. torques ($m = 1$, low n: global modes);
- $+\gamma_0\ \mathcal{B}$: nonlinear feeding from the increase of core modes due to sawtooth crashes, with growth rate $\gamma_0 \propto B^2_{\rm m=1}$;
- $-\alpha_3\ \mathcal{B}^2$: nonlinear damping;
- $-\alpha_4\ \mathcal{V}\ \mathcal{B}$: shear suppression of magnetic turbulence;
- $-\mu_2\ \Delta V/R$: viscous tendency to rigid rotation (R= major radius).

ENHANCED CONFINEMENT TRANSITION

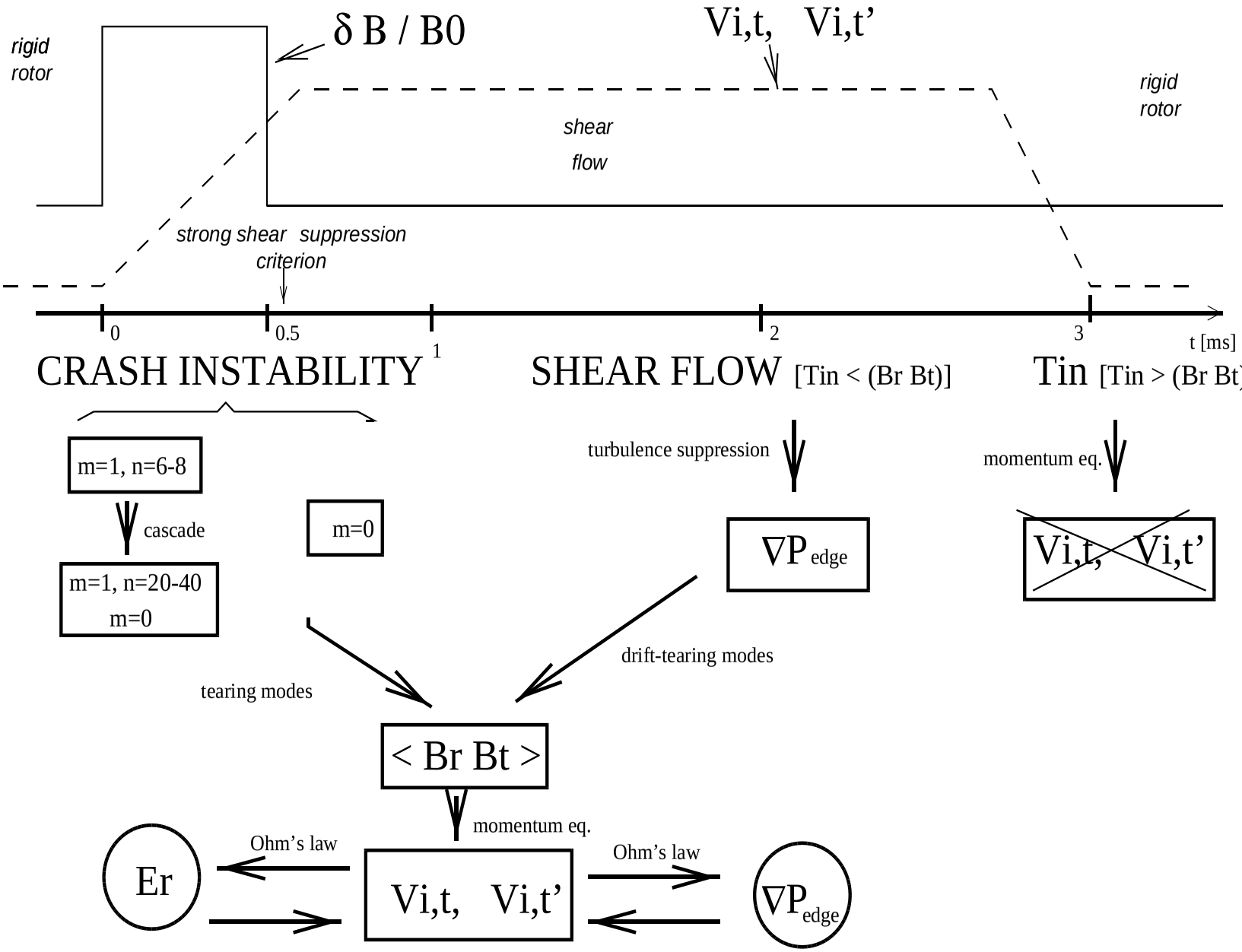

Summary ...

- We are working on a model which describes the dynamics of the spontaneous enhanced confinement regime observed in the Madison Symmetric Torus reversed-field pinch.

- Our model is based on the interplay between the generation of shear flow by turbulence-induced Reynolds stress, and the suppressing action of the flow on the turbulence itself.

  - We study the generation of shear flow by Reynolds stress by solving perturbatively the tearing mode equations in the resistive layer.

  - We study the influence of shear flow on the mode stability by considering the ideal MHD system in cylindrical geometry with an equilibrium flow.

- We present three coupled equations which describe the dynamics of the spontaneous enhanced confinement regime in the RFP.

... and Future Work

- We will perform a bifurcation analysis of the model.

  - Need to complete the shear flow generation calculation;

  - Need to find a simple relation which describes the nonlinear excitation of edge modes due to core modes.

A copy of this poster will be soon available for downloading at "http://sprott.physics.wisc.edu/theory/home.htm"